

Dynamic Nonlinear Response of Super High-Rise Residential Buildings in Urbanized Area During The 2011 off The Pacific Coast of Tohoku Earthquake

M. NAGANO & T. HIDA

Tokyo University of Science, Japan

T. TANUMA & K. WATANABE

Urban Renaissance Agency, Japan



SUMMARY:

Dynamic nonlinear response characteristics of 14 super-high-rise residential buildings in Japan's Kanto and Kansai regions were investigated on the basis of strong motion data recorded during the main shock of the 2011 off the Pacific Coast of Tohoku Earthquake. The structural response of buildings located near the bayside area was larger than that of other buildings at both the base and top floors. Maximum interstory drift angles varied approximately 1/500 rad in Tokyo, and is significant in buildings in the bayside area, where noticeable site amplification in long-period components was recognized. Natural frequencies gradually diminished as the structural response increased from initial levels; reduced frequencies failed to return to their initial levels. The relationship between equivalent inelastic force and these averaged interstory drift angles was evaluated and discussed in this study.

Keywords: Tohoku earthquake, high-rise buildings, recorded motion, natural frequency, temporal variation

1. INTRODUCTION

The Great East Japan Earthquake (Mw9.0)—a massive earthquake in 2011 off the Pacific Coast of Tohoku Earthquake—, shook the eastern region of the Japanese mainland and caused catastrophic damage to buildings along the coastal area, mainly due to the immense force of the resultant tsunami (Architectural Institute of Japan, 2011). The rupture of a large area of a seismic fault led to ground motion of large amplitude and long duration observed in not only in the Tohoku area near the epicenter but also in the Kanto region. Moreover, considerable soil liquefaction occurred in landfilled areas and throughout the alluvial land along the Tone River in Chiba Prefecture (Tokimatsu et al., 2011). Despite being the largest recorded earthquake ever to have struck Japan, structural damages due to ground shaking and collapse appear to have been less severe than expected.

During this earthquake, seismic waves generated by the rupture of the huge seismic fault spread and travelled into the Kanto and Osaka Plains, where thick sedimentary layers exist on the seismic bedrock. They were reflected and amplified within the sedimentary basins and observed the so-called “long-period ground motions,” with long natural periods and durations. Lots of super high-rise residential buildings have been constructed in the highly urbanized area, where the long-period ground motions must have influenced the shaking of those buildings.

The influence of these motions on long-period structures has been the subject of many engineers' interest in Japan since the 2003 Tokachi-Oki earthquake (Mw8.3), Hokkaido. The long-period ground motions observed in the sedimentary Yofutu Plain, far from the epicenter, are considered as one of the plausible reasons for the damage to several oil tanks located in Tomakomai, central part of the Yofutu Plain. The occurrence of the Tokai, Tonankai, and Nankai earthquakes, along the western part of the Japanese archipelago, must have had a serious effect on the dynamic behaviour of the long-period structures densely constructed in the Kanto, Nohbi, and Osaka Plains because of the resonant phenomenon with long durations. Despite these urgent situations, it has been difficult to paint a

precise picture of what will happen to the dynamic behaviour of super high-rise buildings during intense shaking because of a lack of recorded motions.

During the 2011 Tohoku earthquake, strong-motion records were simultaneously obtained at the top, bottom, and middle floors in 14 super-high-rise residential buildings constructed in the Kanto and Kansai regions. All buildings were located within the Kanto and Osaka plains, in which thick sedimentary layers overlie the seismic bedrock, and all buildings experienced long-period ground motion. This study investigates the dynamic nonlinear response characteristics of super-high-rise reinforced concrete buildings on the basis of recorded motion data; in addition, it focuses on maximum structural responses, variations in natural frequencies as well as equivalent curves of the force–displacement relationship.

2. PROFILES OF BUILDINGS

The structures targeted for investigation were 14 super-high-rise residential buildings constructed in the Kanto and Kansai regions. Fig. 1 illustrates the location of these buildings plotted against the contours of the seismic bedrock depth obtained from the Headquarters for Earthquake Research Promotion in 2012. Eight and six buildings in the Kanto and Kansai regions, respectively, were studied. All buildings were located within the Kanto and Osaka plains, in which thick sedimentary layers overlie seismic bedrock. Long-period ground motion during the 2011 Tohoku earthquake is believed to have influenced the dynamic behavior of these super-high-rise buildings.

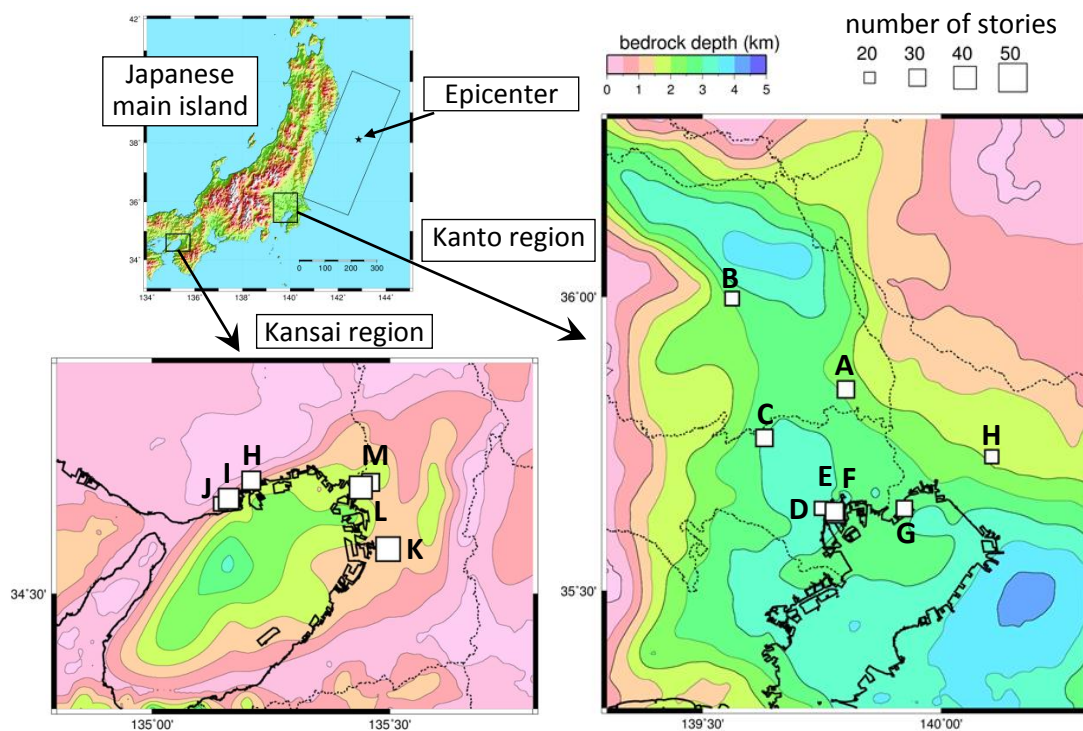


Figure 1. Construction site maps of buildings in the Kanto and Kansai regions investigated in this paper. Plots A–M indicate the building names listed in Table 1.

These buildings were equipped with strong-motion observation systems, and seismic accelerometer records were simultaneously obtained at multiple floor levels: top and first or basement floors, including any mid-level floors. Table 1 lists the profiles, names, number of stories, structural types, and strong-motion observation floors of the buildings. Fig. 2 shows an exterior view of building D and

locations of seismometers.

Most of these buildings are reinforced concrete (RC) structures with more than 24 stories, except for building K [a steel RC (SRC) structure] and building M [a concrete-filled tube (CFT) structure equipped with visco-elastic dampers]. Each building incorporated moment resisting frames with high-strength materials. Most were designed and constructed before 2000.

Table 1. Profiles of buildings examined in this study.

Region	Building names	Stories	Strong-motion observation floors [Floor: (F)]	Region	Building name	Stories	Strong-motion observation floors [Floor: (F)]
Kanto	A	30	B1 F, 15 F, and 30 F	Kansai	I	33	B1 F, 16 F, and 33 F
Kanto	B	25	1 F and 25 F	Kansai	J	37	1 F, 14 F, and 36 F
Kanto	C	30	1 F and 30 F	Kansai	K	25	B1 F, 5 F, and 24 F
Kanto	D	24	B1 F, 12 F, and 24 F	Kansai	L	43	B2 F, 15F, 30 F, and 43F
Kanto	E	33	1 F, 14 F, 24 F, and 32 F	Kansai	M	40	B1 F, 12 F, 26 F, and 40 F
Kanto	F	33	B1 F, 17 F, and 33 F	Kansai	N	31	1 F, 16 F, and 31 F
Kanto	G	28	1 F, 10 F, and 28 F				
Kanto	H	24	1F and 24F				

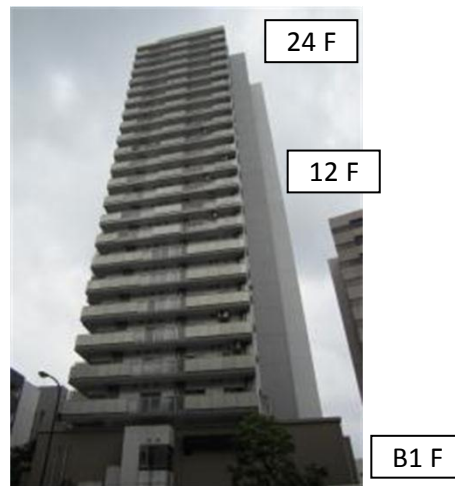


Figure 2. Photograph of building D and locations of accelerographs.

3. STRONG-MOTION RECORDS FROM BUILDINGS

3.1. Accelerograms and response spectra

Fig. 3 shows the accelerograms obtained at the top and basement or ground floors during the main shock of the 2011 Tohoku earthquake. In most of the buildings in the Kanto region, strong motion was recorded with long durations of approximately 10 min, and peak accelerations at the first floors or basements were measured at approximately 100 cm/s^2 . Peak accelerations were amplified by factors of 2–4 at the top floors. Building H showed the highest acceleration because it is located relatively close to the epicenter, at which peak-ground acceleration was significant.

Acceleration levels in the Kansai region were significantly lower than those in the Kanto region because of high attenuation related to the greater distance between Kansai and the epicenter. Structural responses of buildings constructed in the bayside area, buildings M and N, were greater than those in

other areas because ground motion was amplified in the region's soft surface soil.

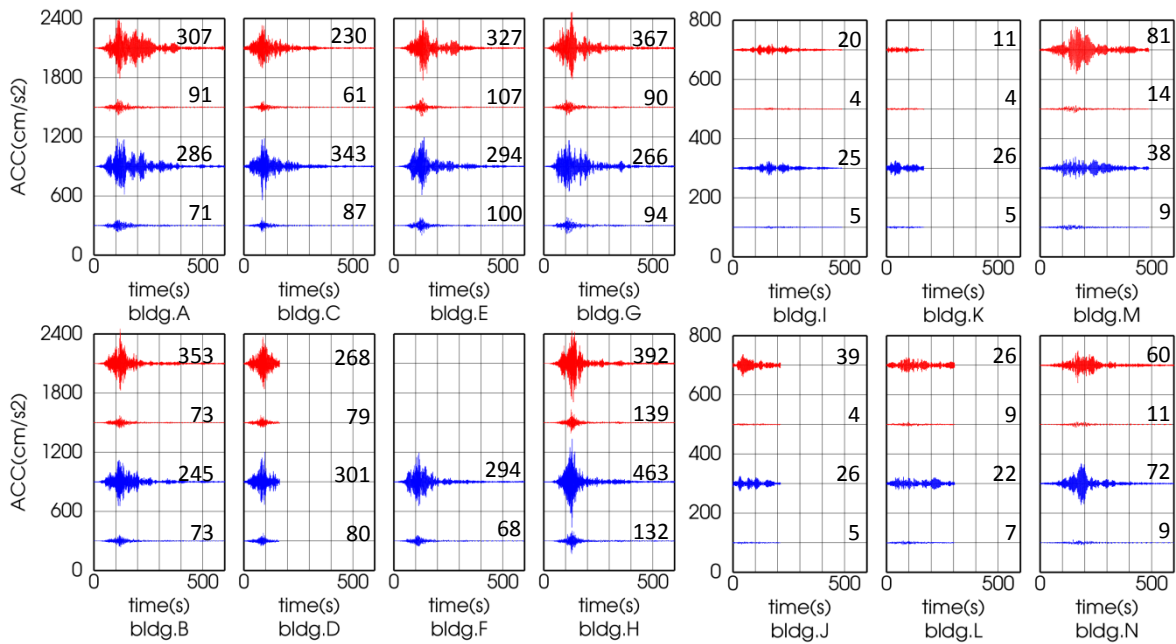


Figure 3. Accelerograms of recorded motion in super-high-rise residential buildings. Upper and lower traces are accelerograms at the top and bottom floors, respectively, along with peak values.

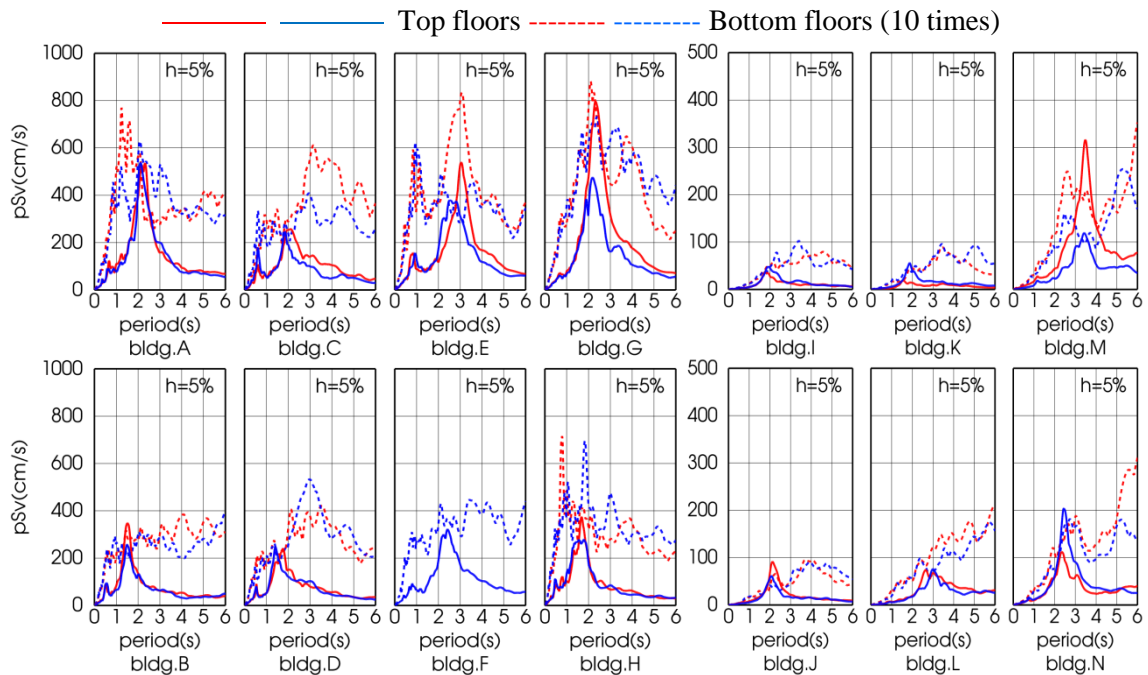


Figure 4. Pseudo-velocity response spectra of recorded motion in super-high-rise residential buildings.

Fig. 4 shows pseudo-velocity response spectra in two horizontal directions for a damping factor of $h = 5\%$. In the Kanto region, spectral amplitudes at the bottom floors were 30–80 cm/s for the period range of 2–3.5 s, corresponding to the natural periods of these buildings. Buildings G and E, located in the Tokyo Bay area, showed large peaks at 2 and 3 s on both the bottom and top floors.

Peak acceleration values were significantly lower in the Kansai region than those in the Kanto region,

in which short-period components of the ground motion were largely attenuated because of Kansai's greater distance from the epicenter. Spectral levels of buildings N and M, located in the Osaka Bay area, were greater than those of the other four buildings. Local-site amplification of long-period ground motion is believed to have affected the structural responses of these buildings. It should be noted that ground-motion amplification occurred not only in a period range of more than 5 s, which is predominant in the Osaka Bay area, but also in the range of 2–3 s.

3.2. Peak floor responses

Distributions of peak-floor accelerations are plotted in Fig. 5(a). The results for each building are plotted in two horizontal directions. In building E, where seismograms were recorded at four separate floor levels, the effect of the second-mode vibration can be measured. This finding indicates that the amplitude of short-period components of ground motion was significant. In the Kansai region, all buildings showed first-mode vibration because long-period components were predominant.

Japan Meteorological Agency's (JMA's) instrumental seismic intensity (I_{JMA}) was evaluated using the recorded data; seismic intensity at each floor is plotted in Fig 5(b). In the Kanto region, I_{JMA} at the first floors or basements varied from 4-lower to 5-lower. At the top floors, the value was amplified to 6-lower or 6-upper. In the Kansai region, I_{JMA} values were generally lower than those in the Kanto region. The increment in I_{JMA} from the bases to the tops of the buildings was approximately 1–1.5 in the two regions.

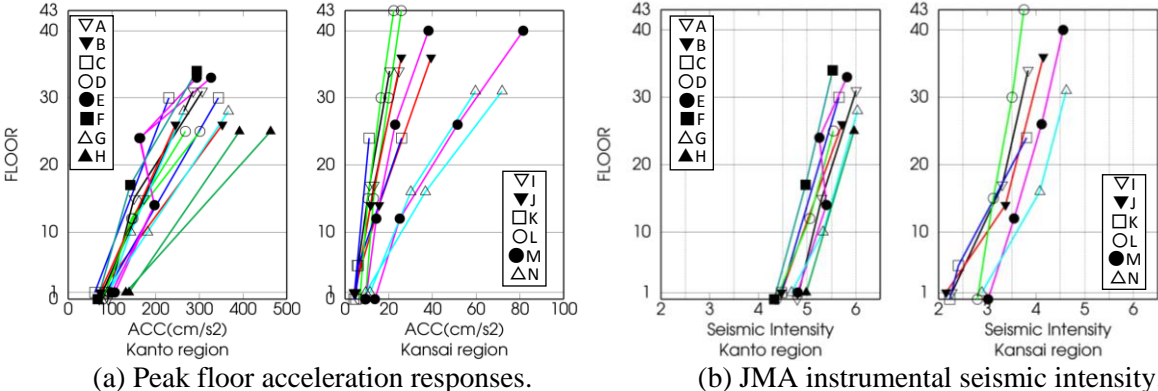


Figure 5. Peak floor acceleration responses and JMA instrumental seismic intensity.

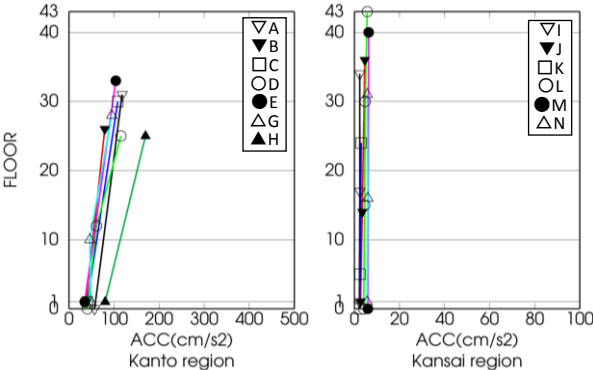


Figure 6. Peak floor acceleration responses in the vertical direction.

Fig. 6 illustrates distributions of peak floor accelerations in vertical directions. Peak UD acceleration levels at the bottom in the Kanto region were approximately half of those in the horizontal directions, whereas the amplification of UD components was smaller than those in the horizontal directions. Vertical accelerations in the Kansai region were significantly smaller than those in the horizontal

direction, and amplification in the top floors did not occur because high-frequency components were largely attenuated due to distance.

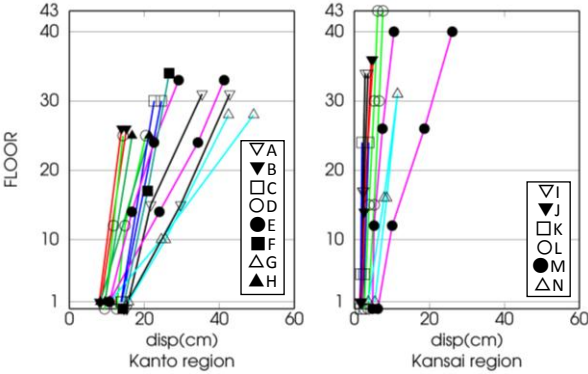


Figure 7. Peak floor displacement responses.

Fig. 7 shows the plot of absolute peak displacement. Top displacement varied by approximately 30 cm in the Kanto region. In the Kansai region, most of the buildings showed a maximum displacement of less than 10 cm. On the contrary, building M, also located in the bayside area, experienced the largest displacement at 26 cm.

The averaged interstory drift angle (IDA) was evaluated from motion data recorded at the top and bottom floors in the Kanto region and is illustrated as 3-D bar graphs in Fig. 8. Two bars indicate the two horizontal directions except building F in which two horizontal records were not obtained. In addition, Fig. 8 also includes peak values of pseudo-velocity spectra between 1.5 and 3.5 s, corresponding to the first natural period during the main shock, obtained from extensive ground-motion records in the Kanto region recorded during the main shock (Nagano, 2012). Dotted lines indicate the coastal area of Tokyo Bay, including the reclaimed land area in which site amplification of long-period ground motion is significant.

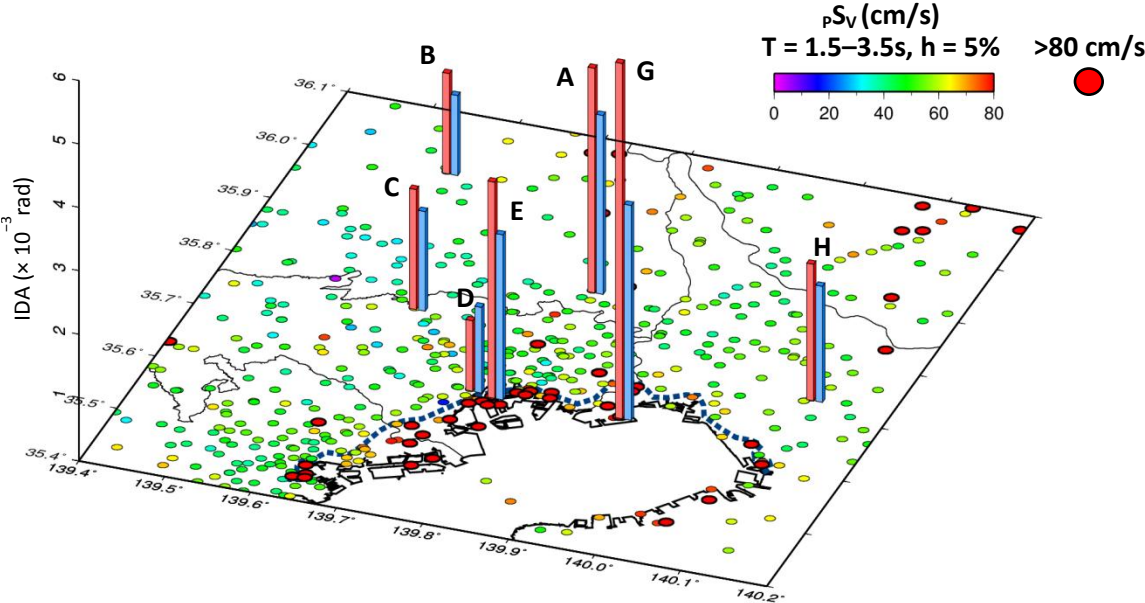


Figure 8. Averaged interstory drift angles in two horizontal directions for buildings in the Kanto region and peak spectral distribution for a period range of 1.5–3.5s evaluated from the extensive ground-motion data.

The maximum IDA of the super-high-rise residential buildings varied by approximately 1/500 rad in the Kanto region. The maximum IDA is significant in Buildings E and G, located in the bayside area,

where noticeable site amplification in long-period components was recognized.

4. VARIATION IN DYNAMIC CHARACTERISTICS DURING MAIN SHOCK

4.1. Temporal variation of natural frequencies

The dynamic characteristics of a reinforced building are known to vary according to the level of input earthquake excitation (Iguchi et al., 2010). Variation in the natural frequencies of RC buildings in this study was investigated using motion recorded on multiple floor levels. The subspace method (Katayama, 2004) was applied to identify the various dynamic characteristics of the buildings during the main shock. Motions recorded at the bottom and other floors, including the top, were used as input and output data, respectively. Signals with a 20-s duration were used for system identification of multiple 10-s intervals. System identification was performed for the two directions separately. Rocking motion at the basement level was included because only horizontal components of the recorded motions were used.

Fig. 9 illustrates temporal variation in fundamental natural frequencies for all buildings over the recorded time in the two horizontal directions. The frequencies were normalized by the initial frequency obtained during the first part of the recorded motions. Moreover, time history of the averaged interstory drift angle (IDA) of the superstructure is traced in the figure. The natural frequencies gradually diminished as the structural response increased from its initial level, which was due to nonlinear behavior such as cracking and yielding of structural members in moment-resistant frames. Natural frequency was reduced by approximately 30% when relative displacement reached its peak. Structural shaking continued for more than 10 min, and the reduced frequencies did not return to their initial levels.

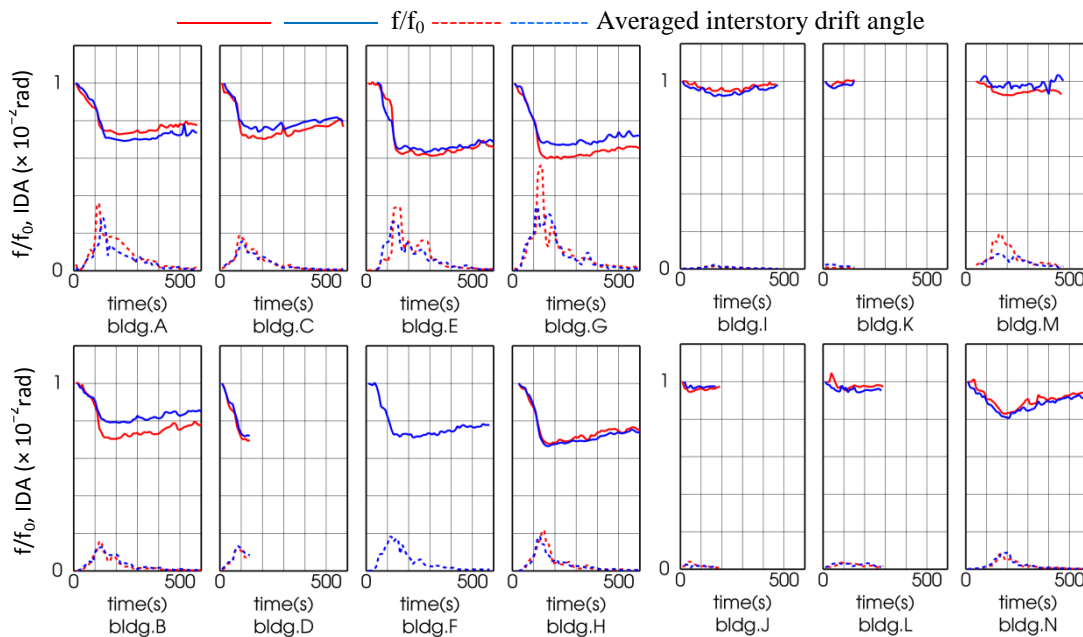


Figure 9. Temporal variation in the fundamental natural frequencies of buildings during the main shock of the 2011 Tohoku earthquake.

Temporal variation in the equivalent damping factor for all buildings is plotted in Fig. 10. Although the identified damping factors are less stable than natural frequencies, several common trends can be recognized. When relative displacement is small, the damping factor is 2%; the frequency gradually increases to 4% or 5% when maximum relative displacement is observed after 150 s. This result is due to hysteric energy consumption accompanied by nonlinearity of RC structural elements.

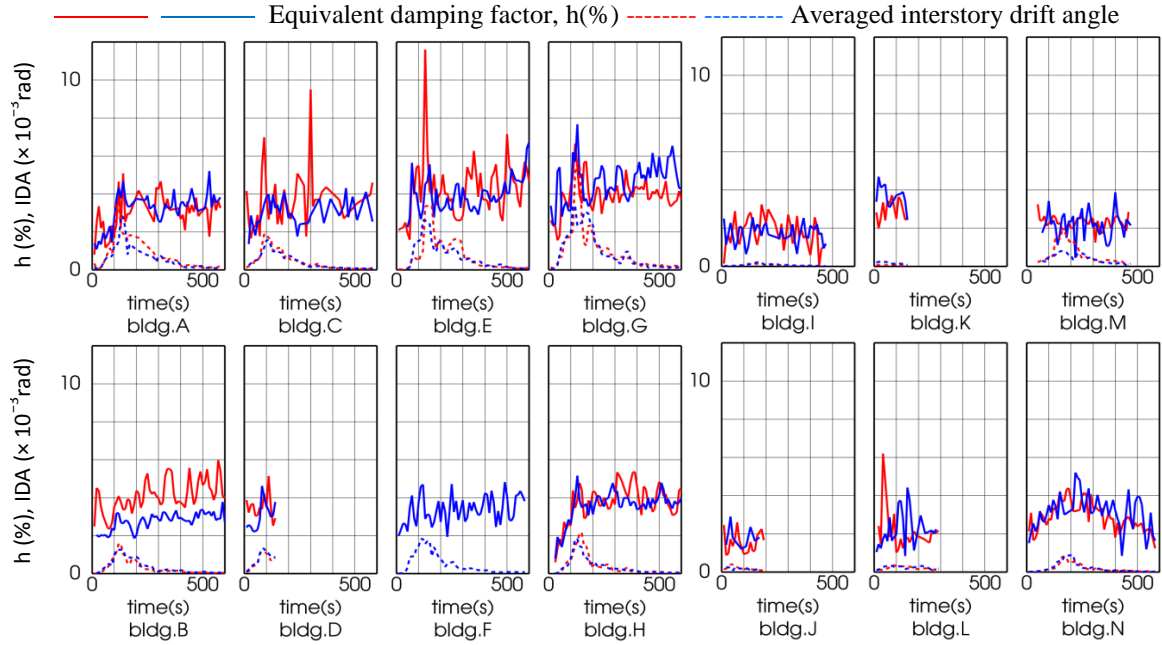


Figure 10. Temporal variation in equivalent damping factors recorded in buildings during the main shock of the 2011 Tohoku earthquake.

4.2. Relationship between equivalent inelastic force and averaged interstory drift angles

Using the temporal data of the natural frequencies f/f_0 and averaged IDA γ in Fig. 9, the normalized force can be evaluated by $q = \gamma(f/f_0)^2$. The quantity q can be interpreted as the total restoring force of the upper structure normalized by initial shearing stiffness G_0A . The relationship between q and γ for all buildings is shown in Fig. 11. Values of q and γ were evaluated for signals with a 20-s duration of multiple 10-s intervals. Dashed lines indicate linear relationship between q and γ , in which the coefficient was obtained from regression; this parameter will be discussed subsequently. Each plot of $q-\gamma$ is interpreted as a steady state response of an inelastic system.

In the Kanto region, first yielding was observed in the loading stage prior to $\gamma = 1 \times 10^{-3}$ rad. After experiencing peak strain level, the $q-\gamma$ relationship showed inelastic loop-like properties in the unloading stage. Energy consumption or the area of the loop increased relative to the peak strain level. Steady-state unloading stiffness was approximately half of that in the loading stage, as indicated by the reduction in the first natural frequency. In the Kansai region, nonlinear behavior was generally small. In Building M, nonlinearity was relatively low despite high strain levels. These results occurred because building M is a CFT structure outfitted with steel beams rather than with reinforced concrete, in which deterioration due to fissures occurs at the two ends of the beam.

On the basis of the available data of q and γ in the loading stage for all buildings in the Kanto region, skeleton characteristics of the $q-\gamma$ relationship are plotted in Fig. 12. The equivalent damping factors $h(\%)$ were also plotted for γ in the loading stage. Most data were well arranged in the $q-\gamma$ curves although variation was relatively high in high-strain levels. Within a small range of the drift angle, the $q-\gamma$ data were plotted linearly. Regression analysis using data $\gamma < 0.88 \times 10^{-3}$ rad indicates $q = 0.845\gamma$ by linear approximation. The coefficient 0.845 indicates the averaged coefficient in the small drift angle range. The reciprocal of the coefficient implies additional stiffness due to nonstructural members in the small amplitude level. In a drift angle range greater than 1.0×10^{-3} rad, stiffness deterioration occurred. Considering that the drift-angle range, shown in Fig. 11, did not reach the yielding level, bilinear approximation can be applied by setting the boundary at $\gamma = 0.88 \times 10^{-3}$ rad.

The bilinear curve after regression analysis in the loading stage is plotted in Fig. 12 as dashed lines. Instant stiffness after cracking was approximately half of the initial stiffness, which appeared to be smaller than that in the structural design. Estimation of the force–displacement relationship from the data of q and γ , on the basis of equivalent properties in the multiple sets of 20-s duration, may lead to some inaccuracy. However, the evaluation of h for γ is less stable than q , and the damping factor h tended to rise as the drift angle increased.

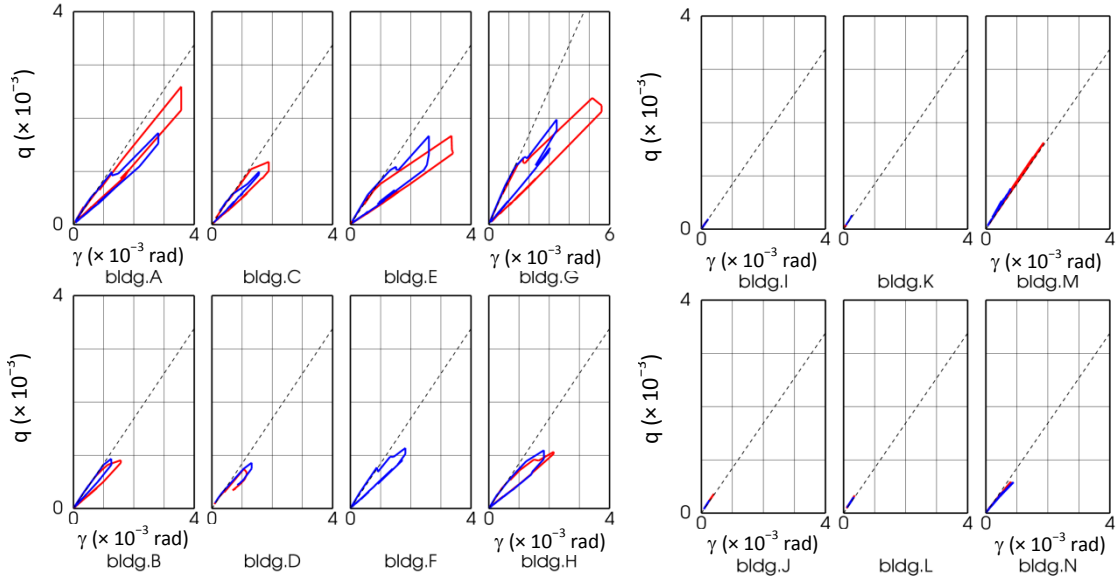


Figure 11. Relationship between equivalent inelastic force and averaged interstory drift angles recorded during the main shock of the 2011 Tohoku earthquake.

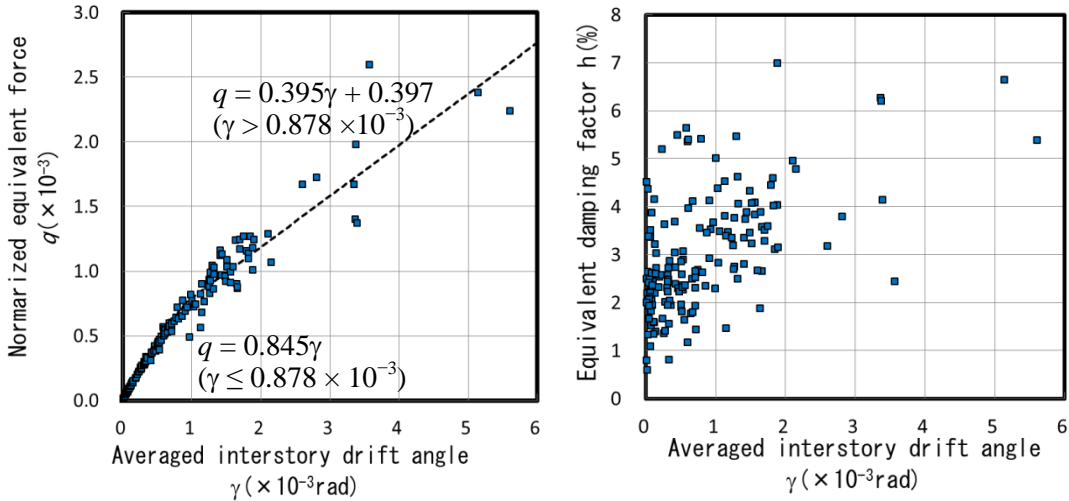


Figure 12. Skeleton characteristics and equivalent damping factors for drift angles.

5. CONCLUSIONS

The dynamic nonlinear response characteristics of 14 super-high-rise residential buildings in the Kanto and Kansai regions were investigated on the basis of motion data recorded during the main shock of the 2011 Tohoku earthquake. The structural response of buildings located near the bayside region was greater than that in other buildings at both the base and top floors. Local-site amplification of ground motion had influenced the structural response of bayside buildings. Maximum interstory drift angles

were varied by approximately 1/500 rad in Kanto region. The building located in the bayside area experienced the largest interstory drift angle. In the Kansai region, most buildings experienced a maximum drift angle of less than 1/1000 rad. However, the building, also located in the bayside region, experienced the largest interstory drift angle at 1/500 rad. Natural frequencies gradually diminished as the structural response increased from initial levels, which was due to nonlinear behavior such as cracking and yielding of structural members in moment-resistant frames. Structural shaking continued for more than 10 min, and reduced frequencies did not return to initial levels. The minimum frequency ratios during the main shock were reduced by 20–40% of the initial event. From the relationship between the normalized force and drift angles obtained from the identification, yielding in the loading stage and inelastic loop-like properties in the unloading stage were detected in the Kanto region. Skeleton characteristics were approximated through a bilinear curve. Instant stiffness after cracking was determined to be approximately half the initial stiffness, which appeared to be smaller than that used in the structural design.

ACKNOWLEDGMENT

The authors would like to express their gratitude to Konoike Construction Co., Ltd., and Obayashi, Kajima, Toda, Hazama, and Maeda corporations, for providing strong motion data for the super high-rise residential buildings during the 2011 off the Pacific Coast of Tohoku earthquake. We also used strong motion records provided by K-NET, KiK-net, JMA, SK-net, MeSO-net, TEPCO, MLIT, BRI, and PARI. The system identification tool developed by Mr. Manabu Kawashima, Sumitomo Mitsui Construction Co., Ltd, is used. A few of the figures in this paper were created by GMT4 (Wessel and Smith, 1998).

REFERENCES

- Architectural Institute of Japan (2011). Preliminary Reconnaissance Report of the 2011 Tohoku-Chiho Taiheiyo-Oki Earthquake. (in Japanese)
- Headquarters for Earthquake Research Promotion. (2012). The prediction maps of the long period ground motions, 2012 version prototype. (http://www.jishin.go.jp/main/chousa/12_choshuki/index.htm, in Japanese).
- Iguchi, M., Kawashima, M., and Kashima, T. (2010). Assessment of Varying Dynamic Characteristics of a SFSI System Based on Earthquake Observation. *Soil-Foundation-Structure Interaction*, Orense, Chouw & Pender (eds), CRC Press, 3–10.
- Katayama, T. (2004). System Identification—Approach from Subspace Methods. Asakura Publishing Co. Ltd. (in Japanese)
- Nagano, M. (2012). 3.1.4 Analysis of Long Period Ground Motions in Metropolitan Area. *Report for Open Workshop on Act against the Long Period Ground Motions*. The Research Subcommittee on Long-Period Structural Responses, Architectural Institute of Japan, 51–58. (in Japanese)
- Tokimatsu, K., Tamura, S., Suzuki, H., and Katsumata, K. (2011). Damages to Soils and Foundations in the 2011 Tohoku Pacific Earthquake. *The 39th Symposium on Earthquake Ground Motions*, Architectural Institute of Japan, 21–34. (in Japanese)
- Wessel, P. and Smith, W.H.F. (1998). New, improved version of the Generic Mapping Tools released. *EOS Trans Am Geophys Union*. **79**. 579